

CrystEngComm

Accepted Manuscript



This is an *Accepted Manuscript*, which has been through the Royal Society of Chemistry peer review process and has been accepted for publication.

Accepted Manuscripts are published online shortly after acceptance, before technical editing, formatting and proof reading. Using this free service, authors can make their results available to the community, in citable form, before we publish the edited article. We will replace this *Accepted Manuscript* with the edited and formatted *Advance Article* as soon as it is available.

You can find more information about *Accepted Manuscripts* in the [Information for Authors](#).

Please note that technical editing may introduce minor changes to the text and/or graphics, which may alter content. The journal's standard [Terms & Conditions](#) and the [Ethical guidelines](#) still apply. In no event shall the Royal Society of Chemistry be held responsible for any errors or omissions in this *Accepted Manuscript* or any consequences arising from the use of any information it contains.

ARTICLE

Simple Growth of BCNO@C Core Shell Fibers and Luminescent BCNO Tubes

Cite this: DOI: 10.1039/x0xx00000x

Liangxu Lin^a, Le Ma^a, Shaowei Zhang^{*b}, Juntong Huang^b and Dan A. Allwood^{*a}Received 00th January 2012,
Accepted 00th January 2012

DOI: 10.1039/x0xx00000x

www.rsc.org/

A novel core shell structure (BCNO@C with C core and BCNO shell) has been prepared using a simple heating reaction. These fibers have a diameter around 100-300 nm with lengths up to hundreds of micrometers. To create BCNO@C fibers, the C fibers (cores) were first grown using Ni particle catalysts before adding BCNO shells. Simple burning of the core shell fibers led to the formation of novel $B_{0.43}C_{0.23}N_{0.27}O_{0.07}$ tubes. Unlike the BCN tubes grown from the substitution of C tubes, the BCNO tubes here have a homogenous structure with luminescence centered at around 386 nm (from 290-700 nm), which was mainly contributed by the 1,3-B centers, carbene structures and BO_2^- species. The method used here is suitable to being adapted in the future to tune the electronic structure of BCN based materials.

1. Introduction

Multilayered hexagonal boron nitride (hBN) nanotubes (BNNTs) and carbon nanotubes (CNTs) are layered materials with densely packed sp^2 hybridized benzene-ring structure in each layer.¹ However, the physical properties of BNNTs and CNTs are greatly different.² Although the preparation of pure BN that displays deep ultraviolet emission is difficult (it is usually suppressed by dopants such as C³), tuning the element composition in the range from hBN to graphite to achieve a $B_xC_yN_z$ structure can open new electronic gaps for various applications (*e.g.* electronics and optoelectronics).⁴

Nevertheless, preparation of $B_xC_yN_z$ nanotubes using arc-discharge,⁵ chemical vapor deposition (CVD)⁶ or pyrolysis techniques⁷ typically involves toxic or expensive reagents such as methane (CH_4), diborane (B_2H_2), ammonia (NH_3) and melamine diborane. The arc-discharge and CVD technologies are also complex and become expensive for $B_xC_yN_z$ nanotube production. Alternative routes may involve the substitution of CNTs with B and N to form doped nanotubes.^{8,9} While the initial growth of CNTs can be expensive, their substitution usually results in a heterogeneous distribution of dopants.^{8,9} Although some new methods, such as electrospinning techniques are well developed for building interesting nanostructures,¹⁰⁻¹² significant works are still need to understanding the deformation of these nanostructures under high temperature conditions (normally involved in the nucleation and growth of inorganic C/BN/BCN fibers).

Here, we report a simple growth route for homogenous and luminescent BCNO tubes. This involves the growth of carbon fibers (catalyzed by Ni particles) followed by the growth of C- and O-doped BN layers around the fibers to achieve a BCNO@C core-shell structure (C core and BCNO shell). $B_{0.43}C_{0.23}N_{0.27}O_{0.07}$ tubes remained after the C cores were burned out and, unlike the other

methods discussed above, had a relatively homogenous B, C, N and O distribution. The C and O dopants in the sp^2 BN lattice creates new luminescent centers and gives much potential for tuning the properties for optical and electronic devices. In this paper, how these interesting structures formed in the reaction is also investigated.

2. Experimental Section

A. Preparation. 2 g VBS750 sealant tape (Tygavac Advanced Materials Ltd) was used as carbon source for the reaction (Scheme S1), which was placed into one side of a corundum tube. An Al_2O_3 boat was used to hold a mixture of B_2O_3 (1 g) and NH_4Cl (4 g). A graphite paper with nickel nitrate coating (0.1 mg/mL $Ni(NO_3)_2$ solution was drop-casted on the substrate with ~ 1 mm thickness, and then dried in the oven) was used to cover the crucible boat. A furnace tube containing the carbon source and Al_2O_3 boat was purged with N_2 for 10 minutes and then heated to 1450 °C (heating rate: 5 °C/min) and held for 1 h in flowing N_2 (purity 99.999%). The fired samples were allowed to cool to room temperature in flowing N_2 . A black layer of product (BCNO@C) was visible on the underside of the graphite paper, which was collected for the characterization and following treatment. Finally, the carbon cores of the collected BCNO@C fibers were removed by heating at 500 °C for 30 minutes in an oven under air condition. As a control, preparation was also conducted without the $Ni(NO_3)_2$ catalyst. For the study of the growth mechanism, the preparation (with $Ni(NO_3)_2$ catalyst) was also conducted at 1000 °C for 1 hour.

B. Characterization. Fourier transform infrared (FT-IR) spectroscopy was performed on a commercial PerkinElmer Spectrum 2000 spectrometer by using a pressed mixture (KBr and resultant product disks). Raman spectra were recorded on a

Renishaw in plus laser Raman spectrometer with an excitation wavelength of 785 nm (with an inVia model microscope and a Streamline Plus system). Scanning electron microscopy (SEM) images were taken by a commercial Inspect-F scanning electron microscope. X-ray diffraction (XRD) pattern was obtained using a Philips PW1830 powder diffractometer (Cu $K\alpha$, wavelength ~ 0.154 nm). Transmission electron microscopy (TEM) images and selected area diffraction patterns (SAED) were taken by a Phillips 420 transmission electron microscope at 120 kV, and by a JEOL 2010F transmission electron microscope operated at 200 kV with field emission gun (for high resolution TEM/HRTEM). Energy-dispersive X-ray spectroscopy (EDS) of the samples were recorded during the SEM (Inspect-F) and TEM (JEOL 2010F) characterizations. The cathodoluminescence (CL) of the sample was recorded by a GatanMono CL-4 CL detector with Inspect-F SEM.

3. Results and discussion

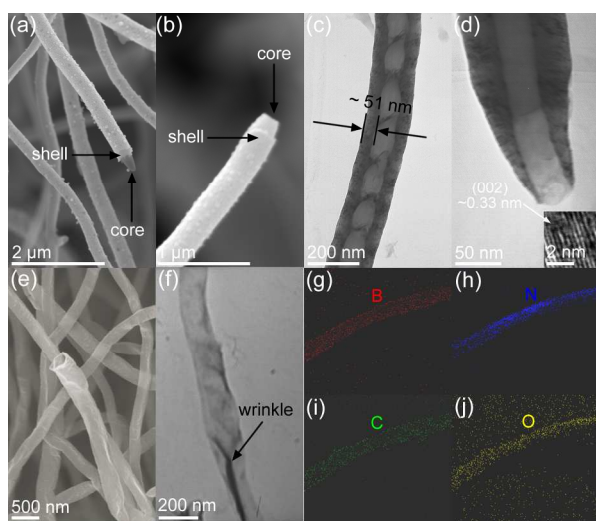


Figure 1. (a, b) SEM and (c, d) TEM images of BCNO@C fibers; (e) SEM and (f) TEM images and (g) B-, (h) N-, (i) C-, and (j) O- EDS maps of BCNO tubes.

Graphite paper prepared with Ni catalyst source was placed over a crucible containing B_2O_3 and NH_4Cl and the crucible heated in a flow of C-containing N_2 gas (Scheme S1; see Experimental Section for further details). SEM of the product that developed on the graphite paper showed fibers with lengths up to hundreds of micrometers (Figures S1&2). These fibers were of 100-300 nm total diameter with a core-shell structure, as observed by SEM and TEM (Figures 1a-d, Figures S2c&d and Figure S3). The shell thickness and core diameter were generally approximately comparable (Figures 1c&d and Figure S3). EDS analyses suggested that cores contained only C and shells B, C, N and O (Figure S4).

It was hard to directly determine the crystallinity of the core due to the large diameter of the BCNO@C fiber. However, XRD of the collected BCNO@C fibers give evident (002) and (100, 101) diffraction peaks of layered materials (graphite, BN and BCNO) at around 26.7 and 43° respectively (Figure S5a). High resolution TEM (HRTEM) of the tip of an exposed core region (Figure 1d inset) shows an interlayer spacing of ~ 0.33 nm, corresponding well with the (002) lattice fringe of graphite (JCPDS card no. 41-1487). The crystallinity of the fiber was further confirmed by the SAED pattern from fiber tip (Figure S5b). The fiber shells are also crystalline, which will be discussed later.

The chemical composition and structure of the BCNO@C fibers were further confirmed by FT-IR and Raman spectroscopies. FT-IR spectra of the fibers (Figure 2a) gave peaks at around 1636 , 1381 , 1107 , 814 and 677 cm^{-1} , which can be assigned to the vibrations from C-C/C=C (also BN-C), B-N, B-O, N-B-O and O-B-O, respectively.¹³ The Raman spectra of the fibers (Figure 2b) showed peaks at around 1347 cm^{-1} (full width at half maximum [FWHM] 115 cm^{-1}) and 1588 cm^{-1} (FWHM 87 cm^{-1}). The first of these corresponds to the D peak of graphite but BN or C/O-doped BN also show a similar peak.⁹ The second peak corresponds to the G peak of graphite.¹⁴ The high intensity ratio of D/G (~ 1.1) is reasonable due to the existence of BCNO structures (B/C/N/O species were from the shell) in the fibers.

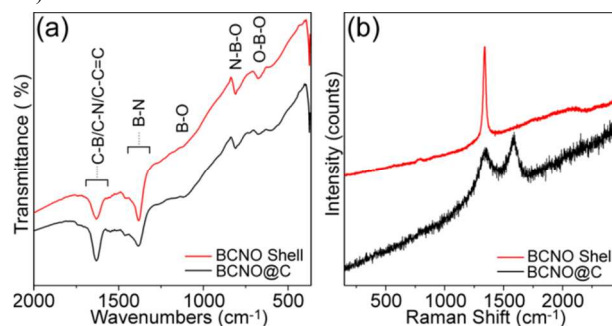


Figure 2. (a) FR-IR and (b) Raman spectra of BCNO@C fibers and BCNO tubes

The carbon core of BCNO@C fibers can be easily removed by heating under air at 550 $^\circ C$ for 30 minutes to leave the BCNO shells as tubes. In contrast with BCNO@C fibers, the formed BCNO tubes collapsed slightly to lose their previous circular cross-section (Figure 1e&f and Figure S6a&b). Correspondingly, the widest diameters of these tubes were slightly larger than that of pristine BCNO@C fibers. The majority of tube tips were flat (Figure 1e and Figure S6a&b) and had the same diameter as the tube's body. However, occasionally, some tips showed horn morphologies (Figures S6c&d).

FT-IR spectra of the hollow BCNO tubes (Figure 2a) showed a weakened and slightly red shifted vibration at around 1626 cm^{-1} (shifted from 1636 cm^{-1} of BCNO@C). It is likely that this is due to the loss of the C-C/C=C contributions with the removal of the C core and that peak was purely due to the C- and O-doped BN structure of the tube. Raman analysis of the BCNO tubes (Figure 2b) confirmed the removal of the C core, with the only response at around 1339 cm^{-1} (FWHM of 29 cm^{-1}) corresponding to a red-shift of the 1365.5 cm^{-1} peak from hBN.¹³ This red shift suggests that C- and O- chemical doping happened within the lateral hexagonal BN structure via substitution of B and N elements rather than the chemical functionalization of the BN structure which, in principle, would suppress the vibration of B-N and lead to blue shifting of the Raman response. Traditional substitution of C tubes (with B and N dopants) normally results in remaining C-C/C=C domains giving a clear Raman response at around 1588 cm^{-1} .⁹ However, the lack of the Raman G peak for C-C/C=C species from our BCNO tubes (Figure 2b) indicates that they contained few carbon-carbon bonds.

TEM observation of a remaining BCNO tube (Figure 1f) shows relatively homogenous contrast when we might expect some areas with wrinkles. This suggests a relatively even spread of the elements in the tube. This is confirmed by the EDS mapping (Figures 1g-j) of one BCNO tube (SEM image of this tube is shown in Figure S7). Further EDS analyses give the average chemical composition of tubes to be $B_{0.43}C_{0.23}N_{0.27}O_{0.07}$ (calculated as an average from ten EDS spectra. Analysis from different areas showed similar chemical composition). The chemical composition of the tube tips and bodies are similar (Figure S8, also similar to the analysis of BCNO shell

before C removal in Figure S4c). The high proportion of C and the absence of a G peak in Raman spectra (Figure 2b) suggest that C distribution is relatively homogenous in the BCNO tubes. Like the C core of the BCNO@C fibers, the BCNO shells are also crystallized. Figure 3 shows HRTEM images of the tubes, which show the crystalline nature of the BCNO. The interlayer distance of the BCNO tubes was measured as around 0.33 nm, corresponding well with the (002) lattice of sp^2 hBN structure (JCPDS card no. 45-0896). However, the HRTEM also suggested some dislocations (e.g. dotted circle in Figures 3a-c) on the wall as well as a crack in the tube (Figure 3d). It is expected since dislocation and crack might be induced by the chemical doping of BN structure and sonication treatment (for TEM analysis), respectively.

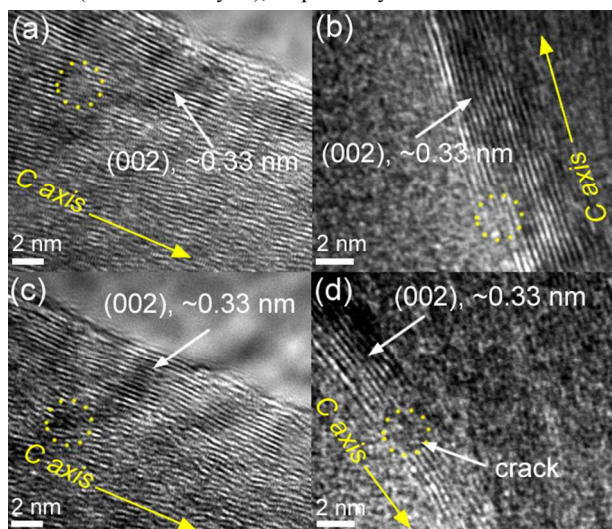


Figure 3. HRTEM images of the BCNO tubes. C axis in these images represents the tube direction, which is parallel to the (002) plane of BCNO tubes.

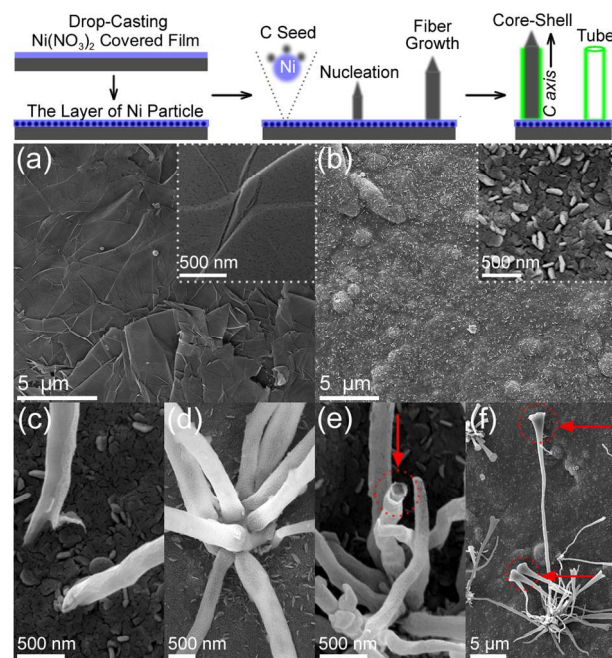


Figure 4. Growth scheme and SEM images of (a) graphite substrate, (b) reacted graphite substrate with Ni catalyst and (c) – (f) various BCNO@C core/shell fibers.

We performed further systematic investigations to understand how these BCNO@C fibers can be grown using this simple method. The

scheme in Figure 4 describes the process of heating the $NiNO_3$ on the graphite substrate to nucleate and form Ni particles ($Ni(NO_3)_2 + C \rightarrow Ni$). The (111) lattice of the crystallized Ni matches that of graphene and has been used previously as a substrate and catalyst for the growth of graphene and graphite fibers/tubes.¹⁵ In our experiment, the growth of fibers was achieved only with the addition of $Ni(NO_3)_2$. The formed Ni particle during the heating process can be the catalyst for the growth of carbon fibers. Figure 4a is an SEM image of the blank graphite substrate, showing the surface morphology (also see Figure 4a inset). Heating the Ni-coated substrates to 1000 °C for 1 h created carbon seeds for form on the substrate surface (the small bright dots in Figure 4b). The Ni particle catalysts gave only a weak signal from EDS (Figure S9), indicating their low presence or perhaps that they are inside the carbon layer. The majority of carbon seeds are plate-like rather than spherical (Figure 4b inset). The crystal structure of graphite means that growth along the (002) plane is much easier than the others; therefore the plate seed can be the host (002) wall for the following growth of carbon fiber (Figure 4c). This deduction corresponds well with SEM and HRTEM observations (Figures 1a-d and Figure 3). Fibres appeared to twist and distort close to their seed before evolving into a cylindrical cross-section (e.g. Figure 4c). Besides, some cylindrical fibers emerging from single larger carbon seeds was also found (Figure 4d).

From these SEM images, it can be concluded that the fibers were grown either from the tip (majority) or building up from the root. Our SEM images shown earlier (Figures 1a & b) suggested that most fibers have a tip diameter smaller than the fiber diameter (also see Figure 4e). This can be explained as the fiber growing by material becoming added to the tip. However, we occasionally found some tips that were much bigger than the diameter of remainder of its fibers (Figure 4f). This is only possible if the fiber was at least in part built up from the root (e.g. Figure S10). Following the formation of carbon fiber, the formed (002) graphite wall performed as the model lattice for the growth of BCNO shell (also see Figure 3). This is understandable since the (002) BN wall (as well as the C and O doped BN) has a similar lattice to graphene and finally led to BCNO tubes as suggested by the growth scheme (see scheme in Figure 4). One short fiber in Figure 4e (dot circled) also clearly confirms that the BCNO shell was co-grown with the C fiber along the (002) orientation (the growth direction has been shown in Figure 3).

From the discussed growth of the BCNO@C fibers, it is interesting to find that the C core was tended to grow with (002) direction (rather than perpendicular to (002)). Many works on the growth of carbon fibers/tubes also gave same feature.⁵⁻⁹ Considering the layered structure of graphite, this is understandable since the nucleation in a graphene layer is easier than the formation of a new layer. The growth of the C fiber with (002) direction, in principle, cannot change the surface energy. However, differentially, like the growth of hBN fiber, growth of the C fiber by attaching new graphene layers increased the surface curvatures and surface energies (the O-containing atoms on the C surface also increased the surface energy of the C core),¹⁶ which increased the affinity of C core with small airborne molecules.¹⁷ Therefore, once the C fiber was formed with a certain diameter, new surfaces with C, B, N, O composites are tended to be formed as the shells. Further precious explanation of this competition growth between C core and BCNO shell may be involved in our future works, which requires systematic investigations of the surface energy of the materials, temperature of the reaction, and the concentration of the supplied gas.

The doping of the BN structure with C and O is likely to cause significant changes to its optical and electronic properties. To investigate this, we performed CL of the obtained BCNO tubes.

Figures 5a-d show SEM and CL images of the BCNO tubes, which were captured during the CL characterization with (Figures 5b-c) and without (Figure 5a) CL beam illumination. CL imaging showed the BCNO tubes to be highly luminescent (Figure 5b), despite their surfaces having been coated with a thin Au layer for SEM imaging. However, the luminescence intensities of the tubes were not homogenous, showing significant contrast in Figure 5b. The CL spectra of two tubes (Figures 5c&d) with different sizes were further analyzed. Both the big and small tubes (indicated in Figures 5c&d) showed similar emission spectra except the intensities which highly depend on their diameter. Luminescence was observed from 290-700 nm, centered at around 390 nm (Figures 5e&f), and composed of one strong peak at around 386 nm (3.2 eV) and three weak emissions at 410 nm (3.0 eV), 438 nm (2.8 eV) and 493 nm (2.5 eV).

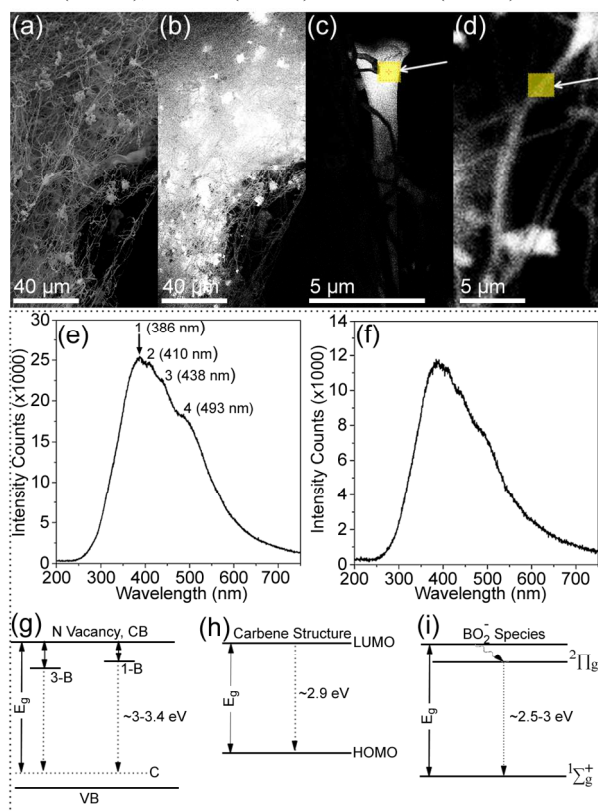


Figure 5. (a) SEM and (b-d) CL images of BCNO tubes. (e,f) CL spectra collected from BCNO tubes, and (g-i) photoluminescence spectra of the BCNO tubes. Spectra in (e) and (f) were collected from the indicated beam position in images (c) and (d), respectively. CB: conduction band, VB: valence band.

On the basis of previous studies, the luminescence here probably arose mainly from the emission centers of carbon-substituted N vacancy point defects (3-B and 1-B centers), BO_x^- ($x = 1$ and 2) species, and carbene structure at zigzag edges. These attributions and energy levels (3.2, 3.0, 2.8, and 2.5 eV) are close to the reported theoretical predictions and experimental findings (emissions from 1,3-B center at around 3.0-3.4 eV, emission from zigzag carbene structure and BO_2^- species at the lower energies 2.7-3.0 eV).^[13,18] Characterization (EDS and FT-IR) shows that the shell is composed of B, C, N and O. Pure hBN domains in the shell did not have such 1,3-B centers. However, 1,3-B centers formed once the N in the BN domain was replaced by C and consist of unpaired electrons trapped in the vicinity of ^{11}B .¹⁸ Electronic transitions from the 1,3-B center to the lower carbon level gives luminescence with energy 3.0-3.4 eV (Figures 5g-i, energy level of 1-B center is slightly higher than that of 3-B center), which is higher than with other luminescent centers

(BO_x^- and carbene structure).^{13,18} This suggests that the main luminescence components at around 386 nm (3.2 eV) and 410 nm (3.0 eV) (Figure 5e) are mainly due to emissions from 1- and 3-B centers, respectively. Besides, the C doping of the pure hBN domain may have led to carbene structure at the zigzag edge, which have emission with energy (Figure 4h, around 2.9 eV) lower than that from 1,3-B center.^{13,18,19} These almost certainly will have been present at tube edges but may also have formed at the dislocations and defects in the tube walls (see Figure 3). The existence of BO_x^- ($x=1,2$) species would also create strong luminescent centers in the tubes. BO_2^- and BO^- are both closed-shell species. BO_2^- has a single emission line (Figure 5i, from first excited state $^2 1 I_g$ to a linear ground state $^1 \Sigma_g^+$, around 2.5-3 eV), whereas BO^- exhibits three well-resolved, equally-spaced lines.^{13,18} The absence of this equally-spaced luminescence in our CL spectra suggests that the emission contribution from BO^- was minimal. Nevertheless, at this stage, it is difficult to differentiate between emissions from zigzag carbene and BO_2^- species as they have similar energies.

4. Conclusion

In summary, we have prepared core shell BCNO@C fibers (diameter of ~100-300 nm and length up to hundreds of micrometers) using a simple heating reaction. Studies show that the carbon fiber (core) grew from the carbon seed (plate), which was catalyzed by Ni particles. In this process, the majority of carbon fibers grew additively from their tip although some appeared to have built up from their root. BCNO layers were grown around the carbon cores to form long core-shell structures. Burning the C core from the structures led to the formation of $\text{B}_{0.43}\text{C}_{0.23}\text{N}_{0.27}\text{O}_{0.07}$ tubes with homogenous element distribution. The tubes showed intense luminescence centered at around 390 nm (from 290-700 nm), which could be identified as emerging from 1,3-B centers, carbene-like zigzag structures and BO_2^- species in the host lattice. Since the electronic structure and luminescence of the tubes are highly dependent on the chemical doping, this growth method has the potential to allow tuning the band structure of BCN and BCNO tubes by changing their composition.

Acknowledgements

This work was supported by the University of Sheffield.

Notes and references

^a Department of Materials Science and Engineering, University of Sheffield, Sheffield S1 3JD, UK.

^b College of Engineering, Mathematics and Physical Sciences, University of Exeter, Exeter EX4 4QF, UK.

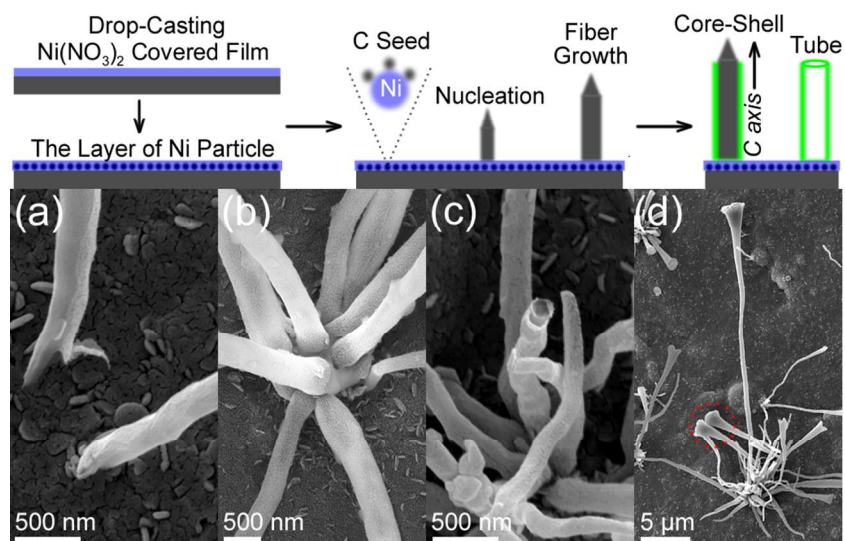
Electronic Supplementary Information (ESI) available: Preparation scheme (Figure S1), SEM images of BCNO@C fibers (Figures S1&2), TEM images of BCNO@C fibers (Figure S3), EDS of the BCNO@C structures under TEM observation (Figure S4), XRD and SAED of BCNO@C fibers (Figure S5), SEM images of BCNO tubes (Figures S6&7), EDS analyses of BCNO tubes (Figure S8), SEM image and EDS analysis of carbon seed (Figure S9) and SEM images of the many fibers grown from one seed (Figure S 10). See DOI: 10.1039/b000000x/

- 1 J. Wang, C. H. Lee and Y. K. Yap, *Nanoscale*, 2010, **2**, 2028; J. Prasek, J. Drbohlavova, J. Chomoucka, J. Hubalek, O. Jasek, V. Adam and R. Kizek, *J. Mater. Chem.*, 2011, **21**, 15872; Y. Yu, H. Chen, Y. Liu, V. Craig, L. H. Li and Y. Chen, *Adv. Mater. Interfaces*, 2014, **1**, 1300002.
- 2 M. R. Roknabadi, M. Ghodrati, M. Modarresi and F. Koohjani, *Physica B*, 2013, **410**, 212.
- 3 Y. Kubota, K. Watanabe, O. Tsuda and T. Taniguchi, *Science*, 2007, **317**, 932.
- 4 T. Lin, C. Su, X. Zhang, W. Zhang, Y. Lee, C. Chu, H. Lin, M. Chang, F. Chen and L. Li, *Small*, 2012, **8**, 1384; J. Lu, K. Zhang, X. F. Liu, H. Zhang, T. C. Sum, A. G. C. Neto and K. P. Loh, *Nat. Commun.*, 2013, **4**, 2681; L. Yin, Y. Bando, D. Golberg, A. Gloter, M. Li, X. Yuan and T. Sekiguchi, *J. Am. Chem. Soc.* 2005, **127**, 16354; E. Lyyamperumal, S. Wang and L. Dai, *ACS Nano*, 2012, **6**, 5259; W. Wang, T. Oqi and Y. Kaihatsu, *J. Mater. Chem.* 2011, **21**, 5183.
- 5 K. Suenaga, C. Colliex, N. Demoncey, A. Loiseau, H. Pascard and F. Willaime, *Science*, 1997, **278**, 653
- 6 L. Yin, Y. Bando, D. Golberg, A. Gloter, M. Li, X. Yuan and T. Sekiguchi, *J. Am. Chem. Soc.*, 2005, **127**, 16354
- 7 S. Wang, E. Lyyamperumal, A. Roy, Y. Xue, D. Yu and L. Dai, *Angew. Chem. Int. Ed.*, 2011, **50**, 1
- 8 Y. K. Yap, *B-C-N Nanotubes and Related Nanostructures*, Springer Dordrecht Heidelberg London New York, **2009**.
- 9 J. Wu, W.-Q. Han, W. Walukiewicz, J. W. Ager, W. Shan, E. E. Haller and A. Zettl, *Nano Lett.*, 2004, **4**, 647.
- 10 S. Agarwal, A. Greiner, J. H. Wendorff, *Prog. Poly. Sci.*, 2013, **38**, 963.
- 11 J. Li, D. Wei, Y. Hu, J. Fang, Z. Xu, *Cryst. Eng. Comm.*, 2014, **16**, 964.
- 12 J. Li, X. Zeng, Y. Dong, Z. Xu, *Cryst. Eng. Comm.*, 2013, **15**, 2372.
- 13 L. Lin, Y. Xu, S. Zhang, I. M. Ross, A. C. M. Ong and D. A. Allwood, *Small*, 2014, **10**, 60.
- 14 L. Lin and S. Zhang, *J. Mater. Chem.*, 2012, **22**, 14385.
- 15 Y. Zhang, L. Zhang and C. Zhou, *Acc. Chem. Res.* 2013, **10**, 2329; C. Che, B. B. Lakshmi, C. R. Martin and E. R. Fisher, *Chem. Mater.*, 1998, **10**, 260.
- 16 D. Chan, M. A. Hozbor, E. Bayramli, *Carbon*, 1991, **29**, 1091.
- 17 L. B. Boivinich, A. M. Emelyanenko, A. S. Pashinin, C. H. Lee, *Langmuir*, 2012, **28**, 1206.
- 18 A. Katzir, J. T. Suss, A. Zunger and A. Halperin, *Phys. Rev. B*, 1975, **11**, 2370; A. Zunger and A. Katzir, *Phys. Rev. B*, 1975, **1**, 2378; J. V. Ortiz, *J. Chem. Phys.*, 1993, **99**, 6727; V. G. Zakrzewski and A. I. J. Boldyrev, *Chem. Phys.*, 1990, **93**, 657; H. Zhai, L. Wang, S. Li and L. Wang, *J. Phys. Chem. A*, 2007, **111**, 1030; J. Agreiter, M. Lorenz, A. M. Smith and V. E. Bondybey, *Chem. Phys.*, 1997, **224**, 301; C. Tang, Y. Bando, C. Zhi and D. Golberg, *Chem. Commun.*, 2007, 4599.
- 19 D. Pan, J. Zhang, Z. Li and M. Wu, *Adv. Mater.*, 2010, **22**, 734; L. Lin and S. Zhang, *Chem. Commun.*, 2012, **48**, 10177.

Graphical Abstract

Simple Growth of BCNO@C Core Shell Fibers and Luminescent BCNO Tubes

Liangxu Lin^a, Le Ma^a, Shaowei Zhang^{*b}, Juntong Huang^b and Dan A. Allwood^{*a}



Synopsis

Homogenous BCNO shell has been grown on C fibers, giving feasible way to achieve BCNO materials with tunable electronic structures.